14 February 2000

PHYSICS LETTERS A

ELSEVIER

Physics Letters A 266 (2000) 19–23

www.elsevier.nl/locate/physleta

A new class of chaotic circuit

J. C. Sprott *

Department of Physics, University of Wisconsin, Madison, WI 53706, USA

Received 30 November 1999; received in revised form 4 January 2000; accepted 4 January 2000
Communicated by C.R. Doening

Abstract

A new class of chaotic electrical circuit using only resistors, capacitors, diodes, and inverting operational amplifiers is described. This circuit solves the equation $\dddot{x} + A\ddot{x} + \dot{x} = G(x)$, where $G(x)$ is one of a number of elementary piecewise linear functions. These circuits are easy to construct and to scale over a wide range of frequencies. They exhibit a variety of dynamical behaviors and offer an excellent opportunity for detailed comparison with theory. © 2000 Published by Elsevier Science B.V. All rights reserved.

PACS: 05.45.Ac; 02.30.Hq; 02.60.Cb; 47.52.+ j; 84.30.Ng
Keywords: Chaos; Electrical circuit; Operational amplifier; Jerk; Differential equations

After three decades of study, the sufficient conditions for chaos in a system of autonomous ordinary differential equations (ODEs) remain unknown. For continuous flows, the Poincaré–Bendixson theorem [1] implies the necessity of three variables and at least one nonlinearity. The Rössler attractor [2] is a standard example of such a system with a single quadratic nonlinearity. Systems with one nonlinearity can generally be written as a third-order ODE in a single scalar variable, suggesting a means to catalog and quantify the complexity of such systems [3]. In this scheme, the Rössler system is relatively complicated [4], and the algebraically simplest dissipative quadratic form [5] is

$$\dddot{x} = -A\ddot{x} + \dot{x}^2 - x, \tag{1}$$

which exhibits chaos for values of A equal to or slightly greater than 2.017. Systems of the form $\dddot{x} = F(\ddot{x}, \dot{x}, x)$ have been called jerk equations (time derivative of acceleration) [6].

The discovery of this and other such simple systems [7] prompted a search [8] for similar examples in which the quadratic nonlinearity is replaced by $|x|$ or another elementary piecewise linear function. Although Eq. (1) with $|\dot{x}|$ in place of $\dot{x}^2$ does not appear to have chaotic solutions for any A and initial conditions, chaos was found [9] in the system

$$\dddot{x} = -A\ddot{x} - \dot{x} + |x| - 1 \tag{2}$$

with A equal to or slightly greater than 0.6. Eq. (2) is a special case of the more general system

$$\dddot{x} + A\ddot{x} + \dot{x} = G(x), \tag{3}$$

where $G(x)$ is a nonlinear function with the properties discussed below. Integrating each term in Eq. (3) reveals that it is a damped harmonic oscillator driven by a nonlinear memory term involving the integral of $G(x)$ [4]. Such an equation often arises in the feedback control of an oscillator in which the experimen-

* Fax: +1-608-2627205.
E-mail address: sprott@juno.physics.wics.edu (J.C. Sprott).

PII: S0375-9601(00)00026-8

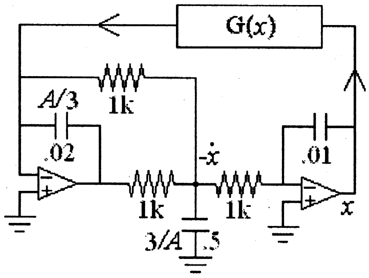

Fig. 1. A general circuit for solving Eq. (3) using one of the nonlinear feedback elements in Fig. 2 for $G(x)$.

tally accessible variable is a transformed and integrated version of the fundamental dynamical variable.

Eq. (3) with a piecewise linear $G(x)$ suggests a class of chaotic electrical circuit that is simple to construct, analyze, and scale to most any desired frequency. It is new in the sense that it does not involve analog multiplication, it uses only resistors, capacitors, diodes and operational amplifiers, and the governing equation is simpler than any previously modeled electronically. The most straightforward implementation [8] involves three successive active integrators to generate $\ddot{x}$, $\dot{x}$, and x from $\dddot{x}$, coupled with a nonlinear element that generates $G(x)$ and feeds it back to $\dddot{x}$. Fig. 1 shows a slightly simpler circuit in which one of the integrators is a passive RC. Above or to the left of each component is the value that would make the circuit behave in real time. Values not shown are unity. Below or to the right are practical values for $A = 0.6$ that produce similar outputs for the op amps and scale the frequency up by a factor of 10^4 into the audio range ($f = 10^4/2\pi \approx 1592$ Hz at the Hopf bifurcation point) so that the bifurcations and chaos can be heard. [1]

In Fig. 1, the element labeled $G(x)$ represents a nonlinear resistor with the feature that the current I exiting the grounded terminal at the left obeys $I = G(V)$, where V is the voltage applied to the terminal at the right. For example, the function $G(x) = B|x| - C$ required to solve Eq. (2) is produced by the circuit in Fig. 2(a) [10]. Fig. 2 shows three other cases with chaotic solutions. In each case, the constant A is taken as 0.6 and B is selected to be well

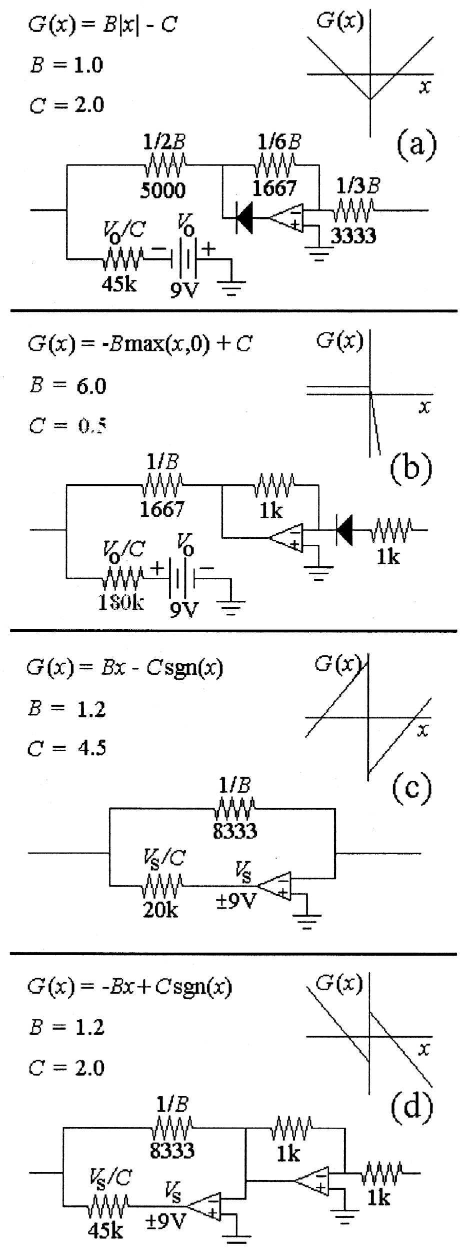

Fig. 2. Some nonlinear forms for $G(x)$ that produce chaos and circuits to produce them.

[1] More detail on a circuit that solves Eq. (2), including a sound file of the bifurcations as $1/A$ is increased can be found at http://sprott.physics.wisc.edu/chaos/abschaos.htm.

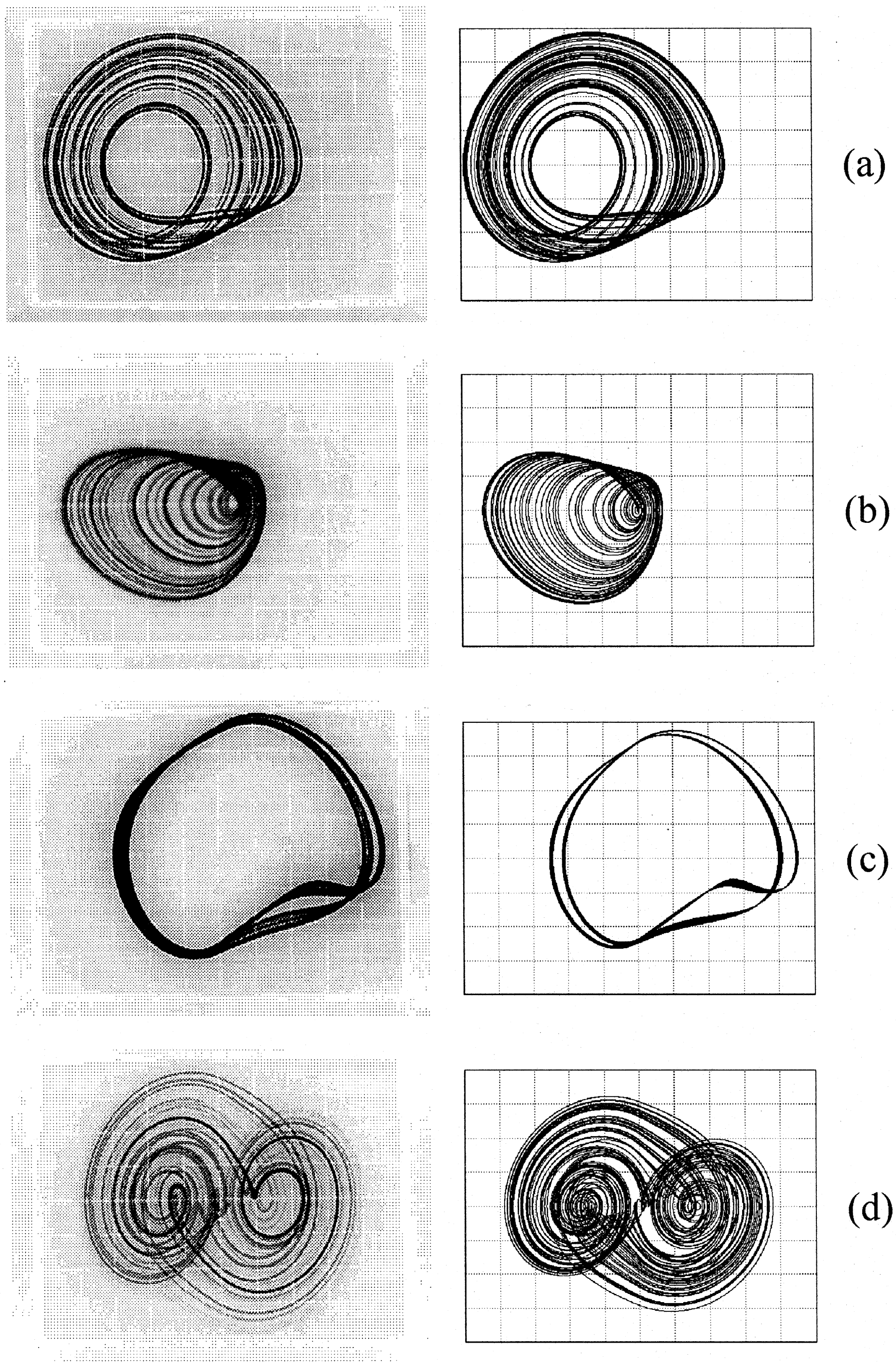

Fig. 3. Chaotic attractors produced by each of the circuits in Fig. 2 in the $x - \dot{x}$ plane. In the left-hand column are oscilloscope traces, and in the right-hand column are the corresponding numerical solutions on the same scale

into the chaotic regime. The constant C determines the size of the attractor and has been adjusted for each case so that x reaches a maximum value of slightly less than 5. Such a voltage is well above the noise level but comfortably below a value that would typically saturate the op amps.

Most any of the components can be varied to serve as a bifurcation parameter. Unfortunately, there is no single parameter that controls A in any of the circuits or B in the circuit in Fig. 2(a), but the resistor in the lower right of Fig. 1 can be made variable with resistance R. With the capacitors chosen to give $A = 0.6$ for $R = 1$, the trajectory in $A - B$ space then follows the curve $A = 0.4 + 0.2/R$, $B = 1/R$.

These circuits are similar in spirit to Chua's circuit [11,12], which uses two capacitors, an inductor, and diodes with operational amplifiers or transistors to provide a piecewise linear approximation to a cubic nonlinearity. Chua's circuit has a much more complicated representation in terms of $\dddot{x}$ with many more than four terms, involving step functions, delta functions, and their products with derivatives of x. Because of the delta functions, the dynamics are not continuous in the space of $(x, \dot{x}, \ddot{x})$. Since the contraction is not constant along the trajectory, it is more difficult to verify the Lyapunov exponents. Chua's circuit is more difficult to construct, scale to arbitrary frequencies, and analyze because of the inductor with its frequency-dependent resistive losses. Three reactive components (capacitors or inductors) are required for chaos in systems with continuous flows so that the Kirchhoff representation of the circuit contains three, first-order ODEs.

These circuits provide three points of detailed comparison with theory – the frequency of oscillations, the values of A and B at which the various bifurcations occur, and the amplitude of the output voltage $x(t)$. All three agree with numerical calculations to within the precision of the electrical components (typically 10%). A version of the circuit in Fig. 2(a) was constructed with high precision components ($\sim 1\%$), and it was verified that the frequency and amplitude agree with numerical calculations to within a few percent. The onset of chaos occurred for a value of R about 12% smaller than expected, however. The reason for this discrepancy is that this particular implementation of the absolute value circuit requires an operational amplifier with a large slew rate to minimize hysteresis near the bend in the curve. This problem can be circumvented by operating at a lower frequency or by using a slightly more complicated version of the absolute value circuit. Fig. 3 shows oscilloscope traces in the $x - \dot{x}$ plane of the attractors produced by each of the systems in Fig. 2 for the parameters listed along with the corresponding numerical prediction, plotted on the same scale.

The system in Eq. (3) with a nonlinear $G(x)$ has been relatively little studied. Coulett, Tresser, and Arneodo observed chaos in numerical simulations with a cubic [13] and a special piecewise linear [14,15] form of $G(x)$, and Rul'kov, et al. [16,17] devised an RLC circuit using an unspecified nonlinear amplifier to produce a particular form of $G(x)$. It does not appear to be generally known that many functions $G(x)$ produce chaos, some examples of which are listed in Table 1. These systems are elementary, both in the sense of having the algebraically simplest autonomous ODE and in the form of the nonlinearity. The table lists typical values of B that give chaos for arbitrary values of C with $A = 0.6$, along with the numerically calculated largest Lyapunov exponents (LE) in base-*e*. The other Lyapunov exponents are 0 and $-(\text{LE} + A)$, and the Kaplan–Yorke dimension [18] is $D_{KY} = 2 + \text{LE}/(\text{LE} + A)$. Other chaotic systems can be found in which $G(x)$ is a delta function or a hysteretic (multivalued) function, in which case only a second-order ODE is required for chaos.

Table 1
Some simple functions $G(x)$ that produce chaos in Eq. (3) with $A = 0.6$. The constant C is arbitrary and only effects the size of the attractor.

$G(x)$	B	LE (base-*e*)
$\pm(B\|x\| - C)$	1.0	0.036
$-B\max(x,0) + C$	6.0	0.093
$Bx - C\,\mathrm{sgn}(x)$	1.2	0.657
$-Bx + C\,\mathrm{sgn}(x)$	1.2	0.162
$\pm B(x^2/C - C)$	0.58	0.073
$Bx(x^2/C - 1)$	1.6	0.103
$-Bx(x^2/C - 1)$	0.9	0.126
$-B[x - 2\tanh(Cx)/C]$	2.2	0.221
$\pm B\sin(Cx)/C$	2.7	0.069
$\pm B\cos(Cx)/C$	2.7	0.069

For bounded solutions, $G(x)$ must average to zero along the orbit [9], which means that any continuous $G(x)$ must have at least one zero at $x = x^*$. The stability of the fixed point at $(x^*, 0, 0)$ is determined by the solutions of the eigenvalue equation $\lambda^3 + A\lambda^2 + \lambda - G' = 0$, where $G' = \mathrm{d}G/\mathrm{d}x|_{x^*}$. This point is locally stable for $-A \leq G' \leq 0$ and undergoes a Hopf bifurcation at $G' = -A$, where $\lambda = \pm i$. Thus, one would expect chaotic systems of this form to require a nonlinearity with either a positive slope at its zero crossing, or a sizeable negative slope, implying a negative resistance in the corresponding circuit model. Systems with $G' > 0$ apparently require at least two fixed points for chaos, but systems with $G' < -A$ only need one. All the cases studied have these features. A scaling that preserves G' and the shape of $G(x)$ only effects the size of the attractor.

Of the cases studied, the largest Lyapunov exponents occur for systems with $G(x) = Bx - C\mathrm{sgn}(x)$. Using a variant of simulated annealing, the parameters A and B were adjusted to maximize the Lyapunov exponent. The result was $A = 0.55$ and $B = 2.84$, for which the Lyapunov exponents (base-e) are $(1.055, 0, -1.655)$, giving an attractor with a Kaplan–Yorke dimension of $D_{\mathrm{KY}} = 2.637$. The attractor is contained within a thin torus that nearly touches the boundary of its small basin of attraction so that initial conditions must be chosen carefully to produce bounded solutions. This case resembles the one shown in Fig. 3(c).

It is also interesting to determine the least nonlinear form of $G(x)$ for which chaos occurs, which we take to mean the two-part piecewise linear function with the smallest bend at the knee, θ. Of the cases studied, this condition occurs for $G(x) = \pm(B|x| - C)$ with $A = 0.025$ and $B = 0.468$, for which $\theta(= 2\tan^{-1}B)$ is about 50.2°. The basin of attraction is very small, and the chaotic attractor coexists with a nearby limit cycle.

Circuits of this type are well suited for detailed quantitative testing of bifurcation theory and other chaotic properties. They may have practical application in secure communications and broadband signal generation since they are especially simple circuits whose properties can be predicted and controlled with very high accuracy.

Acknowledgements

I am grateful to Stefan Linz, Lucas Finco, and Tom Lovell for useful discussions and to Mikhail Reyfman and Nicos Savva for constructing a precision version of the circuit.

References

[1] M.W. Hirsch, S. Smale, Differential Equations, Dynamical Systems and Linear Algebra, Academic, New York,,1974.
[2] O.E. Rössler, Phys. Lett. A 57 (1976) 397.
[3] R. Eichhorn, S.J. Linz, P. Hänggi, Phys. Rev. E 58 (1998) 7151.
[4] S.J. Linz, Am. J. Phys. 65 (1997) 523.
[5] J.C. Sprott, Phys. Lett. A 228 (1997) 271.
[6] H.P.W. Gottlieb, Am. J. Phys. 64 (1996) 525.
[7] J.C. Sprott, Am. J. Phys. 65 (1997) 537.
[8] J.C. Sprott, Am. J. Phys., in press.
[9] S.J. Linz, J.C. Sprott, Phys. Lett. A. 259 (1999) 240.
[10] R.J. Wincentsen, EDN 17, 44, November 1, 1972.
[11] T. Matsumoto, L.O. Chua, M. Komoro, IEEE Trans. Circuits Syst. CAS 32 (1985) 797.
[12] T. Matsumoto, L.O. Chua, M. Komoro, Phys. D 24 (1987) 97.
[13] P. Coullet, C. Tresser, A. Arnéodo, Phys. Lett. A 72 (1979) 268.
[14] A. Arneodo, P. Coullet, C. Tresser, Commun. Math. Phys. 79 (1981) 573.
[15] A. Arneodo, P. Coullet, C. Tresser, J. Stat. Phys. 27 (1982) 171.
[16] N.F. Rul'kov, A.R. Volkovskii, A. Rodríguez-Lozano, E. Del Río, M.G. Velarde, Int. J. Bifur. Chaos 2 (1992) 669.
[17] E. Del Río, M.G. Velarde, A. Rodríguez-Lozano, N.F. Rul'kov, A.R. Volkovskii, J. Bifur. Chaos 4 (1994) 1003.
[18] J. Kaplan, J. Yorke, in: H.O. Peitgen, H.O. Walther (Eds.), Functional Differential Equations and the Approximation of Fixed Points, Lecture Notes in Mathematics 730 Springer, Berlin,), 1979, p. 204.